한국전기전자재료학회 추계학술대회 논문집 1997

원자로 모의 다공질 매체의 유효 열전달 계수 측정

Measurement of the Effective Thermal Conductivity of Porous Media in the Mockup Apparatus of Reactor Vessel

김 용 균, 황 종 선°, 이 용 범, 최 석 기, 남 호 윤
Y.K. Kim, J.S. Hwang, Y.B. Lee, S.K. Choi, H.Y. Nam

한국원자력연구소
Korea Atomic Energy Research Institute

Abstract

Temperature distribution measurements in the mockup apparatus of reactor vessel were performed to determine the effective thermal conductivity of Al powder porous media where stainless steel tubes were installed with different geometry. The temperature distributions at four separated sections with different arrangements of porous media have different slopes according to the geometrical configuration. From the measured temperature distribution, effective thermal conductivity have been derived using the least square fitting method.

I. INTRODUCTION

The Advanced Liquid Metal Reactor (ALMR) plant has three redundant methods for shutdown heat removal: 1) the normal heat transport system including the primary and secondary sodium systems, steam generator system, and condenser; 2) an Auxiliary Cooling System(ACS) which removes heat from the core by natural convection in the primary and intermediate systems; and 3) a safety related Reactor Vessel Auxiliary Cooling System(RVACS) which removes heat passively from the reactor vessel. The RVACS can dissipate all of the reactor decay heat through the reactor and containment vessel walls to the ambient air sink by the inherent processes of natural convection in fluids, heat conduction in solids, thermal radiation heat transfer, and convective heat transfer.

The thermal performance of the RVACS is self-regulating and depends solely on the reactor temperature, i.e. the heat removal rate is low during normal operation conditions (0.7MWth), as desired, and increases to about 2.5MWth at peak performance in the case of ALMR Mod-A[1]. A number of experiments and associated analyses have been performed to evaluate the long-term natural convection heat transport from the core to the rather distributed heat sink provided by the reactor vessel and air-side heat transfer to naturally convection cooling air in the ducts[2-6]. In order to apply this new concept more generally to all Liquid Metal Reactors (LMRs), the feasibility study should be performed through experiments and verified computer codes.

And the porous medium approach is one of the calculation methods which are used in the thermo-hydraulic analysis of reactor vessel. The porous medium formulation requires permeability,

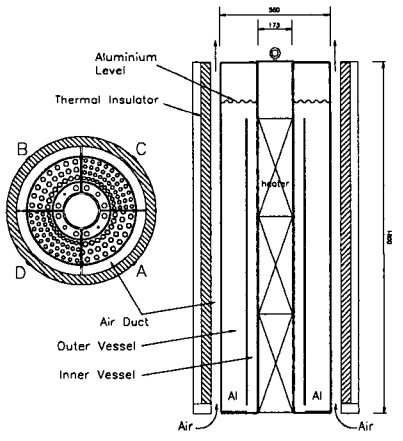

Fig. 1. Schematic diagram of natural heat removal test facility using aluminium.

distributed resistance and distributed heat source, which are closely related to the geometric configuration of the problem. Since four different tube arrangements have been employed in our experiment, the present experimental data may provide a good data set for the validation of computer code based on porous medium approach.

The objectives of this work are to determine the effective thermal conductivity of various geometrical porous media and to obtain the experimental data for the heat transfer processes by natural convection occurring in the air duct.

II. EXPERIMENTS

A. Experimental Apparatus

A schematic diagram of the experimental apparatus is shown in Fig. 1. It consists of three major parts : (1) annular cylindrical vessel (1.8m in height, 0.175m inside diameter, and 0.56m outside diameter), (2) three electrical heaters installed at center and controlled individually (30kW maximum total power), and (3) air duct for cooling the vessel wall by natural convection (0.05m air gap). The annular vessel is filled with 200 mesh aluminium powder and divided into two vessels, inner vessel and outer vessel. In the outer vessel, several stainless tubes containing air are installed for different porosities.

Also the vessel is separated into four sections using thermal insulator. Four sections have four different geometrical structures with combinations of tube sizes(0.0191m and 0.0254m outside diameter) and arrangements(triangle and rectangle), respectively. But total inner tube areas of four sections are same.

For temperature measurement, 184 K-type thermocouples were installed in the experimental apparatus. Tests of all thermocouples have been performed to know the temperature uncertainties at boiling water before installation. The uncertainties

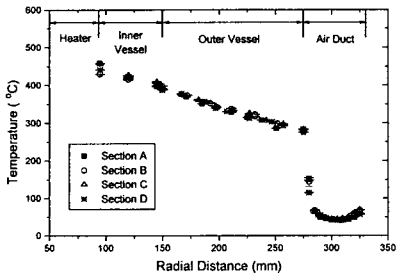

Fig. 2. Typical temperature distribution measured at H=750mm, Q=7.5kW.

of the selected thermocouples did not exceed ± 0.2℃. The 152 thermocouples in the vessel were fixed at measure positions with radial arrangement at the three heights, H=250, 750, and 1250mm. However the 32 thermocouples in the air duct were movable to radial direction.

B. Experimental Procedure

The experiments have been conducted varying the heater power rates at steady and transient conditions. It takes more than ten hours to reach the steady state which was defined with the variation of saturated temperatures in vessel less than 1℃/hr.

The heater power rate (Q) was varied from 1.5kW to 9kW with a step of 1.5kW. When a steady state was reached at each power rate, we acquired 100 temperature data sets of 184 thermocouples during 3000 seconds with an interval of 30 seconds. And the temperature distributions in the air duct were scanned using 32 radially movable thermocouples with a 5mm step. At 10 positions, we obtained air temperature data during 200 seconds with 10 second interval, respectively.

III. RESULTS AND DISCUSSION

A. Mean Temperature

From the measured data, mean temperature values have been obtained for six heater power rates. Fig. 2 shows the typical mean temperature distribution of the present experiment, which was measured at the H=750mm points in the condition of Q=7.5kW. Experimental errors have been estimated from the statistical errors and the uncertainties of thermocouples given by manufacturer (±0.5℃).

This result shows that temperature is a function of radius. The distributions at four sections show similar tendency and the differences among sections are not significantly discriminative in Fig. 2. But the distributions at outer vessel region are different as expected. The differences will be analysed in the following part of the present report.

B. Effective Conductivity Of Outer Vessel

The outer vessel is filled with porous media and the heat conduction depends on the structure and the thermal conductivity of each phase. For the analysis of the macroscopic heat flow through heterogeneous media, the effective thermal conductivity $\langle k \rangle = k_e$ is used.

When a temperature gradient exists in a body,

Table 1. Fitted parameter output at H=750mm

P, kW	Section A		Section B		Section C		Section D	
	k_1	k_2	k_1	k_2	k_1	k_2	k_1	k_2
1.5	0.0258	0.5277	1.542E-8	3.1912	1.593E-8	3.1653	1.275E-8	3.3309
3.0	0.00698	3.3134	7.274E-8	4.0338	8.250E-9	3.9500	1.045E-8	4.1743
4.5	0.00963	1.5140	0.00221	3.3386	1.088E-8	3.9291	8.139E-9	4.0178
6.0	0.00900	1.0009	0.00623	1.8879	0.01163	0.4377	0.00177	3.5281
7.5	0.00937	1.0012	0.00867	1.2481	0.01708	-1.3088	0.00669	2.2965
9.0	0.00972	0.4540	0.00945	0.4805	0.01923	-3.0734	0.00987	0.7969

the energy transferred by conduction is described as following equation[7]:

$$q = -k_e A \frac{\partial T}{\partial x} \quad (1)$$

where q is the heat-transfer rate, A is the cross-sectional area, and $\frac{\partial T}{\partial x}$ is the temperature gradient in the direction of the heat flow.

In the present experiment of steady state, we analysed the temperature data with an assumption of azimuthal independence. Also we assumed that the amount of the net heat flow in the longitudinal direction was negligible with respect to that in the radial direction i.e. $q \simeq q_r$ at H=750mm. Since k_e can be approximated to a first order function of temperature, we can write a more simplified form of above equation as follows:

$$q_r = -k_e A \frac{dT}{dr}, \qquad k_e \simeq k_1 T + k_2 \quad (2)$$

where k_1 and k_2 are the appropriate constant coefficients in a specific temperature region.

From the equation (2), T can be solved analytically as a function of radial distance r as follows:

$$T = \sqrt{\frac{-q_r}{\pi h k_1} \ln r/r_0 + (T_0 + k_2/k_1)^2} - k_2/k_1 \quad (3)$$

where r_0 and T_0 are the values at the outer surface of wall separating the inner vessel and the outer vessel, and h is the height of the vessel.

In Fig. 3, the typical temperature distributions in the outer vessel has been plotted for the radial distance at Q=7.5kW and H=750 mm. This figure shows that the slope of temperature distribution varies according to the difference of geometrical structures among four sections. To quantify this difference, k_1 and k_2 coefficients in the above equation of T have been obtained using least square fitting method. In the figure, curves represent the fitted temperature. The fitted parameter output for various heater power rates at H=750 mm have been obtained and listed in Table 1.

From the analysis of experiment, we can see that heat transfer capabilities of four sections are different according to the geometrical structure of porous media. Further analysis and generalization of this phenomena are in progress.

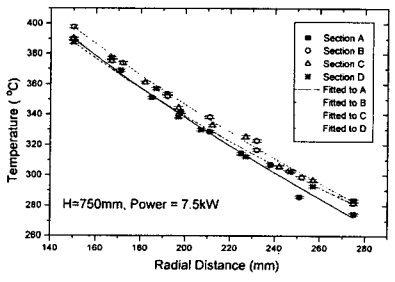

Fig. 3. Temperature distributions in the outer vessel at H=750 mm, Q=7.5kW.

C. Heat Transfer In The Air Duct

The experiments were carried out varying the total power from 1.5kW to 9.0kW. In the case of vertical flat plates, it appears that the plate can be taken to be covered by a turbulent boundary layer if $Ra_L \geq 10^9$ and the temperature profile obeys the 1/7th power-law turbulent distribution as follows[8,9]:

$$\theta \equiv \frac{T(r) - T_\infty}{T_w - T_\infty} = 1 - \eta^{1/7} \quad (4)$$

where

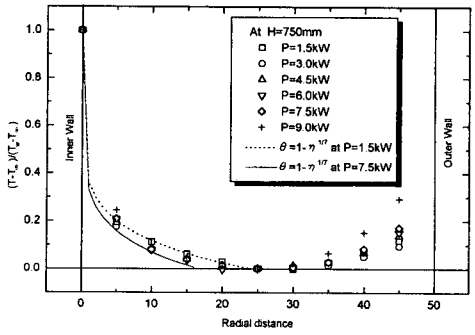

Fig. 4. Temperature distributions in the air duct.

$$\eta = \frac{r}{C_2 H^{1/4}}, \quad C_2 = \frac{4(15/16)^{1/4}(1+20/21\,\mathrm{Pr})^{1/4}}{[g\beta(T_w - T_\infty)\,\mathrm{Pr}/\nu^2]^{1/4}}. \quad (5)$$

In the above equations, Pr represents the Prandtl number and ν the kinematic viscosity.

In the Fig. 4 the experimental temperature distributions and the temperature profile obtained from the 1/7th power-law distribution and the integral method are plotted. Error bars are not displayed because they are very small compared to the symbol. From the figure the experimental data agree well with the solution.

In fig. 5 the Nusselt number was plotted according to the Grashof number. In the figure the obtained heat transfer data were compared with Shin correlation[9] and Siegel one[10]. Present data are slightly higher than Siegel's correlation which is used for the case of vertical wall uniform heat flux in air natural convection. The reason of this result could be explained that the values of Nu calculated from the present experimental data contains the natural convection effect as well as radiation one. As a result, the correlation was derived as follows:

$$Nu_x = 7.28\ \mathrm{Gr}_x^{0.146}. \quad (6)$$

IV. CONCLUSION

The experiments to determine the effective thermal conductivity of porous media with different geometry and to obtain the experimental data for the heat transfer process by natural convection were carried out. The following conclusions can be drawn from the test results.

(1) The temperature distributions of four sections have different slopes. The value of effective thermal conductivity derived from the distribution using the least square fitting method are also different according to the geometrical arrangement.

(2) The results in the air duct show that it is possible to remove the heat at maximum heater power of 3.4 kW/m^2 by the natural convection

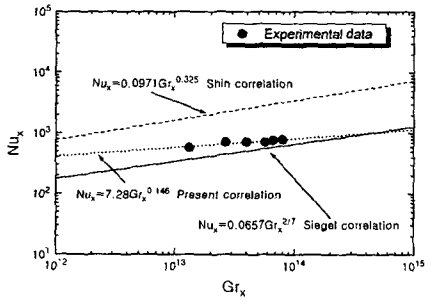

Fig. 5 Comparison of present data and others for air natural convection.

from the outer wall to the air. And also the temperature distributions in the air duct agree well with the 1/7th power-law turbulent temperature distribution. The obtained heat transfer data have been compared with the existing correlations.

REFERENCES

[1] A. Hunsbedt, "Experiments and Analyses in Support of the U.S. ALMR Thermal-Hydraulic Design," IWGRF/88 Specialists' Meeting on Evaluation of Decay Heat Removal by Natural Convection, Oarai Engineering Center, PNC, Japan, pp.97-118 (1993).

[2] Y. Nishi and I. Kinoshita, "Syudy on Reactor Vessel Auxiliary Cooling System with High-Performance Heat Collector," Fast Reactor and related Fuel Cycle, Proc. Int. Conf. Kyoto, Vol. P3, pp.12.6-1.

[3] I. Maekawa and M. Nakaoji, "A Study on the Decay Heat Removal Capability of a Reactor Vessel Auxiliary Cooling System," IWGFR/88 Specialists' Meeting on Evaluation of Decay Heat Removal by Natural Convection, pp.67-77, Oarai Engineering Center, PNC, Japan (1993).

[4] J.J. Oras, et al., "Results of ANL's Thermal-Hydraulic Test Program Supporting PRISM: Phase I and Phase II," Proc. Int. Topical Meeting on Safety of Next Generation Power Reactors, May 1-5, 1988, Seattle, WA (1988).

[5] R. Johnson and R. Soucy, "ETEC Testing of Passive Decay Heat Removal Systems," 4th Int. Topical Meeting on Thermal Hydraulics (Proc., Kalsruhe, 1989) Vol.I, pp.336-371, NURETH-4 (1989).

[6] J.C. Guzak, et al., "Analysis of the Natural Convective Air Cooling Tests in the FFTF Interim Decay Storage Vessel," ASME-JSME Thermal Engineering Joint Conference (Proc. Honolulu 1987) Vol.III, pp.497-502 (1987).

[7] J.P. Holman, Heat Transfer, McGraw-Hill, Inc., pp.2-6 (1976).

[8] A.J. Ede, "Advances in Free Convection," Adv. Heat Transfer, 4, pp.1-64 (1967).

[9] J.J. Shin, R.C. Lotti, and R.F. Wright, "NPR and ANS Containment Study Using Passive Cooling Techniques," Proceedings of the 8th KAIF/KNS/OKAEA Anunal Conference, Seoul, pp.91-99 (1993).

[10] L.C. Burneister, Convective Heat Transfer, John Wiley & Sons, pp.538-545 (1982).